Electronic Supplementary Information

Hydroxylated non-fullerene acceptor for highly efficient inverted perovskite solar cells

Qing Yang,[a,b] Xuan Liu,[a] Shuwen Yu,[a] Zhendong Feng,[a,b] Lixin Liang,[a,b] Qin Wei,[a] Youyang Wang,[c] Xiaobo Hu,[c] Shaoqiang Chen,[c] Zhaochi Feng,[a] Guangjin Hou,[a] Kaifeng Wu,[a] Xin Guo,[a] and Can Li*[a]*

[a] State Key Laboratory of Catalysis, Dalian Institute of Chemical Physics, Chinese Academy of Sciences, Dalian National Laboratory for Clean Energy, Dalian 116023, China.

[b] University of Chinese Academy of Sciences, Beijing 100049, China.

[c] Department of Electronic Engineering, East China Normal University, Shanghai 200241, China.

* E-mail: guoxin@dicp.ac.cn; canli@dicp.ac.cn

Experimental Section

Materials

The patterned indium tin oxide (ITO) glass substrates (15 Ω sq^{-1}), lead (II) iodide (PbI_2, 99.999%) and Formamidinium iodine (FAI) were purchased from Advanced Election Technology CO., Ltd. Methylammonium bromide (MABr) was purchased from the Greatcell Solar. Cesium iodide (CsI, 99.99%), lead (II) bromide ($PbBr_2$, 99.99%) and poly[bis(4-phenyl)(2,4,6-trimethyphenyl)amine] (PTAA) were purchased from Xi'an p-OLED Corp.. The [6,6]-phenyl-C61-butyric acid methyl-ester (PCBM) were purchased from Solarmer Energy Inc.. SnO_2 colloid precursor (tin (iv) oxide, 15% in H_2O colloidal dispersion) was purchased from Alfa Aesar. Other organic solvents and materials used for device fabrication were purchased from Sigma-Aldrich and used as received.

Device fabrication and characterization

Preparation for solution: The PTAA was dissolved in 1 mL toluene with 1.5 mg mL^{-1} stirring over 3 hours. The $Cs_{0.05}(FA_{0.83}MA_{0.17})_{0.95}Pb(I_{0.83}Br_{0.17})_3$-based perovskite precursor solution was prepared by dissolving FAI (1 M), PbI_2 (1.1 M), MABr (0.2 M), $PbBr_2$ (0.2 M) and CsI (0.05 M) in a mixture solvent of dimethylformamide (DMF) and dimethyl sulfoxide (DMSO) (4:1 volume/volume) and stirred overnight at room temperature. 1.4 M FAI, 1.4 M PbI_2, and 0.07 M CsI were dissolved in the same mixture solvent with stirring at 60 °C for 2 h to prepare the $Cs_{0.05}FA_{0.95}PbI_3$-based perovskite precursor solution. A 0.45 μm PTFE filter was used to filter the perovskite precursor solution before fabricating device.

Device fabrication: The 1.5 cm×1.5 cm ITO-coated glass substrates were cleaned by sonication in acetone, isopropanol (IPA) and ethanol subsequently for 30 min each, followed by ultraviolet-ozone treatment for 20 min. The PTAA solution was spin-coated at 4000 rpm for 30 s and then annealed at 100 °C for 10 min in the nitrogen filled glove box. When the substrates cooled to room temperature, 100 μL DMF was spin-coated on the PTAA layer at 4000 rpm for 30 s to improve the wettability of perovskite precursor solution on PTAA layer. Then the $Cs_{0.05}(FA_{0.83}MA_{0.17})_{0.95}Pb(I_{0.83}Br_{0.17})_3$-based or $Cs_{0.05}FA_{0.95}PbI_3$-based perovskite precursor solution was deposited onto the PTAA layer by a consecutive two-step spin-coating procedure at 1000 rpm and 5000 rpm for 10 s and 40 s, respectively. During the second step, the substrate was treated by drop-casting 200 μL chlorobenzene (CB) or IT-DOH (or ITIC) in CB (0.5 mg mL^{-1}) at the end of 20 s, respectively. The $Cs_{0.05}(FA_{0.83}MA_{0.17})_{0.95}Pb(I_{0.83}Br_{0.17})_3$-based perovskite and $Cs_{0.05}FA_{0.95}PbI_3$-based perovskite films were annealed at 105 °C for 60 min and 150 °C for 15 min, respectively. Noted that most of characterizations were conducted based on the $Cs_{0.05}(FA_{0.83}MA_{0.17})_{0.95}Pb(I_{0.83}Br_{0.17})_3$ (CsFAMA) perovskite to verify the validity of the IT-DOH treatment method, and the $Cs_{0.05}FA_{0.95}PbI_3$ (CsFA) perovskite was employed to prove the universality of this method and to obtain a higher PCE. After cooling down to the room temperature, the PCBM (20 mg mL^{-1} in CB) and bathocuproine (BCP, 0.5 mg mL^{-1} in IPA) were sequentially spin-coated at 1000 rpm for 30 s and 4000 rpm for 30 s, respectively. Finally, 100 nm silver was thermally

evaporated under 3×10^{-4} Pa through a shadow mask to define the valid area of 0.04 cm^2.

Solar cell characterization: The current density–voltage (J−V) measurement was performed (2400 Series SourceMeter, Keithley Instruments) *via* the solar simulator (SS-F5-3A, Enlitech) along with AM 1.5G spectra whose intensity was calibrated by the certified standard silicon solar cell (SRC-2020, Enlitech) at 100 mW cm^{-2}. The external quantum efficiency (EQE) data were obtained by using the solar-cell spectral-response measurement system (QE-R, Enlitech). The J–V measurements were carried out in nitrogen-filled glove box. The devices were measured both in reverse scan (1.3 V→ -0.1 V, step 0.02 V) and forward scan (-0.1 V→ 1.3 V, step 0.02 V). The device stability tests were carried out in a nitrogen-filled glove box, and the devices were unencapsulated under continuous one-sun light illumination or in the dark with a temperature of 25 °C.

Instrumentations and characterizations

Photo-induced force microscope (PiFM) images were measured by a VistaScope from Molecular Vista Inc. operated in dynamic mode using commercial gold-coated silicon cantilevers (NCHAu) from Nanosensors. The excitation laser is a Laser Tune IR Source from Block Engineering. Fourier transform infrared (FTIR) spectra were collected using micro-ATR mode with Broker Optics Hyperion 3000. Scanning electron microscopy (SEM) images were taken by a Quanta 200F microscope (FEI Company) with an accelerating voltage of 10 kV. Steady photoluminescence (PL) and time-resolved PL (TRPL) spectra were recorded on an FLS920 fluorescence

spectrometer (Edinburgh Instruments) in air at room temperature. The excitation wavelength of PL is 550 nm. And the TRPL measurements were performed using time-correlated single photon counting (TCSPC) with a 406.8 nm laser. The 2D ^{1}H-^{1}H DQ/SQ spectrum was acquired using a solid state NMR spectrometer (wide-bore 14.10 T AVIII 600 with a 3.2 mm HXY probe) at magic angle spinning frequency of 22 kHz, and the DQ coherence was excited by back-to-back sequence with 181.8 μs mixing time. [1] The ^{1}H NMR measurement in solution was carried out on the Bruker AVANCE III 400 (400 MHz) spectrometer at room temperature. The spectra were referenced on the internal standard TMS. In order to eliminate the interference of water, the IC-OH and PbI_2 materials were dried at 65 °C in a vacuum oven for 12 hours to remove the water as much as possible. Moreover, new deuterated DMSO was used as NMR solvent to dissolve the IC-OH and PbI_2 just before the ^{1}H NMR mearsurement. X-ray photoelectron spectroscopy (XPS) analysis was carried out on a Thermo Esclab 250Xi photoelectron spectroscopy with a monochromatic Al Kα X-ray radiation as the X-ray source for excitation and normalized to the C 1s peak (284.6 eV) for the sample. Femtosecond transient absorption spectra (TAS) were recorded by using an ultrafast TA spectrometer (Time-Tech Spectra, femtoTA100) based on a regenerative amplified Ti:sapphire laser system from Coherent (800 nm, 35 fs, 6 mJ/pulse, and 1 kHz repetition rate), nonlinear frequency mixing techniques and the Helios spectrometer S3. For the measurements of thermal admittance spectroscopy, perovskite solar cells were placed in a cryostat (Janis Ltd. CCS-150) inside through an air-cooled Helium compressor. The measurement was performed by

an Agilent 4284A LCR meter within a temperature range of 180-330 K in darkness. The amplitude of the AC modulation voltage was controlled at 25 mV (rms) to maintain a linear response with modulation frequency varied from 20 Hz to 1 MHz with an increment of $10^{0.1}$ Hz. The applied DC bias voltage was kept at 0 V during the measurement. Grazing-incidence wide-angle X-ray scattering (GIWAXS) measurements were carried out at the Shanghai Synchrotron Radiation Facility (SSRF) with an incident photon energy of 10 keV (a wavelength of 1.2398 Å) at an incident angle of 0.3° and an exposure time of 15 s. The structure of samples for the GIWAXS measurement is glass/ITO/PTAA/control or IT-DOH-treated perovskite prepared as the same method for devices. Electrochemical impedance spectroscopy was implemented on the complete PSCs using a CIMPS-4 system (ZAHNER PP211) controlled by Thales measurement software.

The trap density (N_t) by SCLC method can be calculated through the following equation:

$$N_t = \frac{2\varepsilon\varepsilon_0 V_{TFL}}{eL^2}$$

where e, L, ε_0 and ε are the elementary charge, the perovskite thickness, the vacuum permittivity and the relative dielectric constant (46.9 for triple-cation perovskite), respectively.[2]

To investigate the P_{in} dependence of V_{oc} by using the following equation:

$$V_{oc}(P) = \frac{nkT}{q}\ln(P) + C$$

where the *k*, T, q, n and C are the Boltzmann constant, the temperature in Kelvin, the elementary charge, the ideal factor related to the dominant recombination mechanism in devices and the constant, respectively.

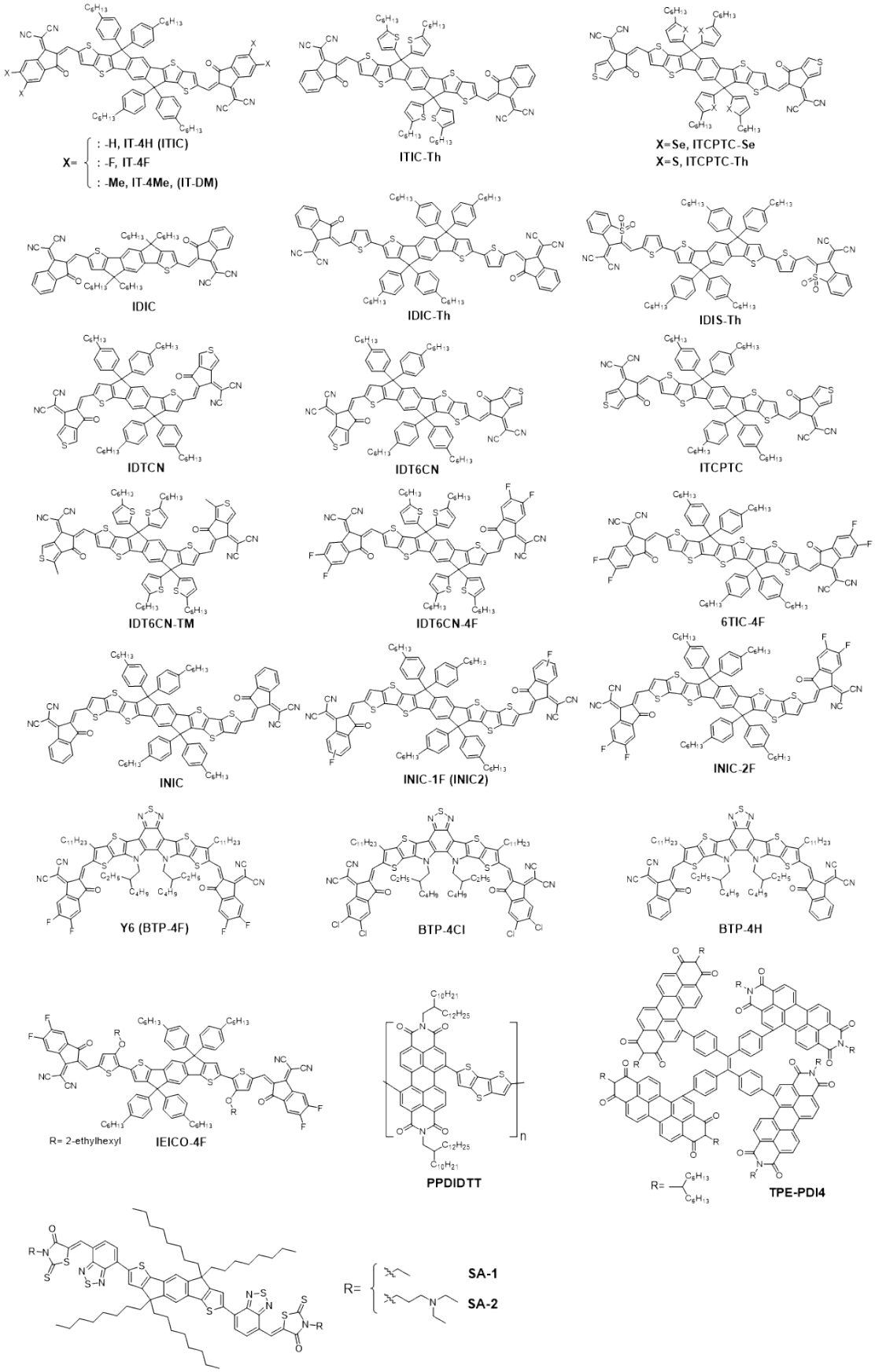

Fig. S1 Molecular structures of reported NFAs employed in PSCs.

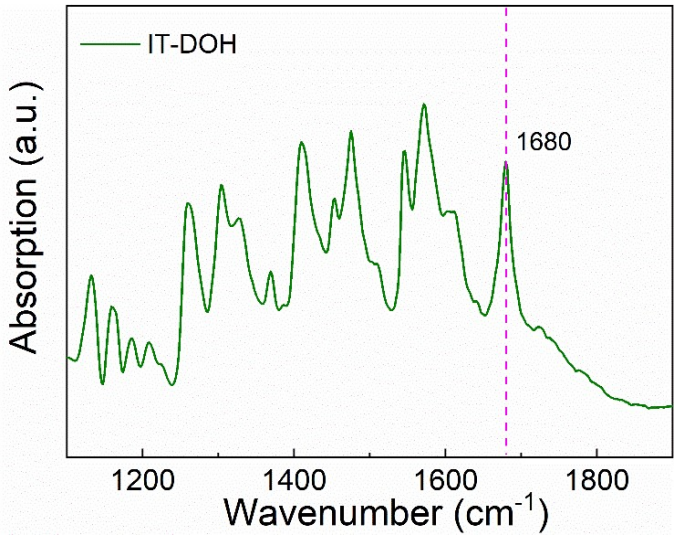

Fig. S2 FTIR spectrum of IT-DOH neat film.

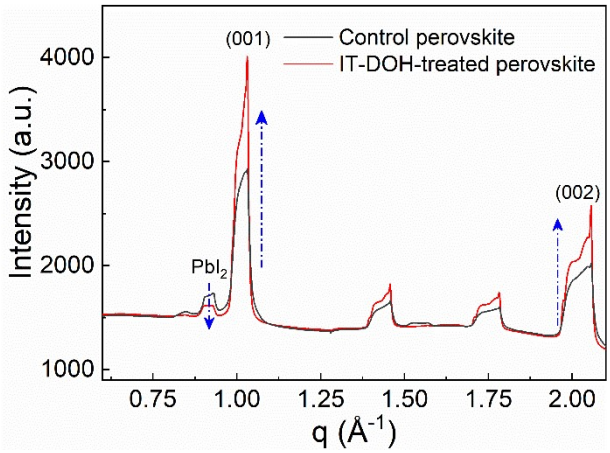

Fig. S3 Line-profile extracted from the 2D GIWAXS images of control and IT-DOH-treated perovskite films, respectively.

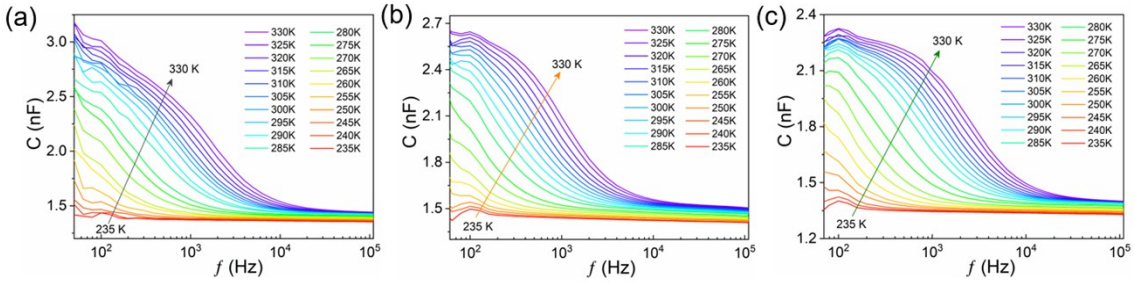

Fig. S4 Temperature-dependent C–*f* curves of (a) control, (b) ITIC-treated and (c) IT-DOH-treated PSCs based on the CsFAMA, respectively.

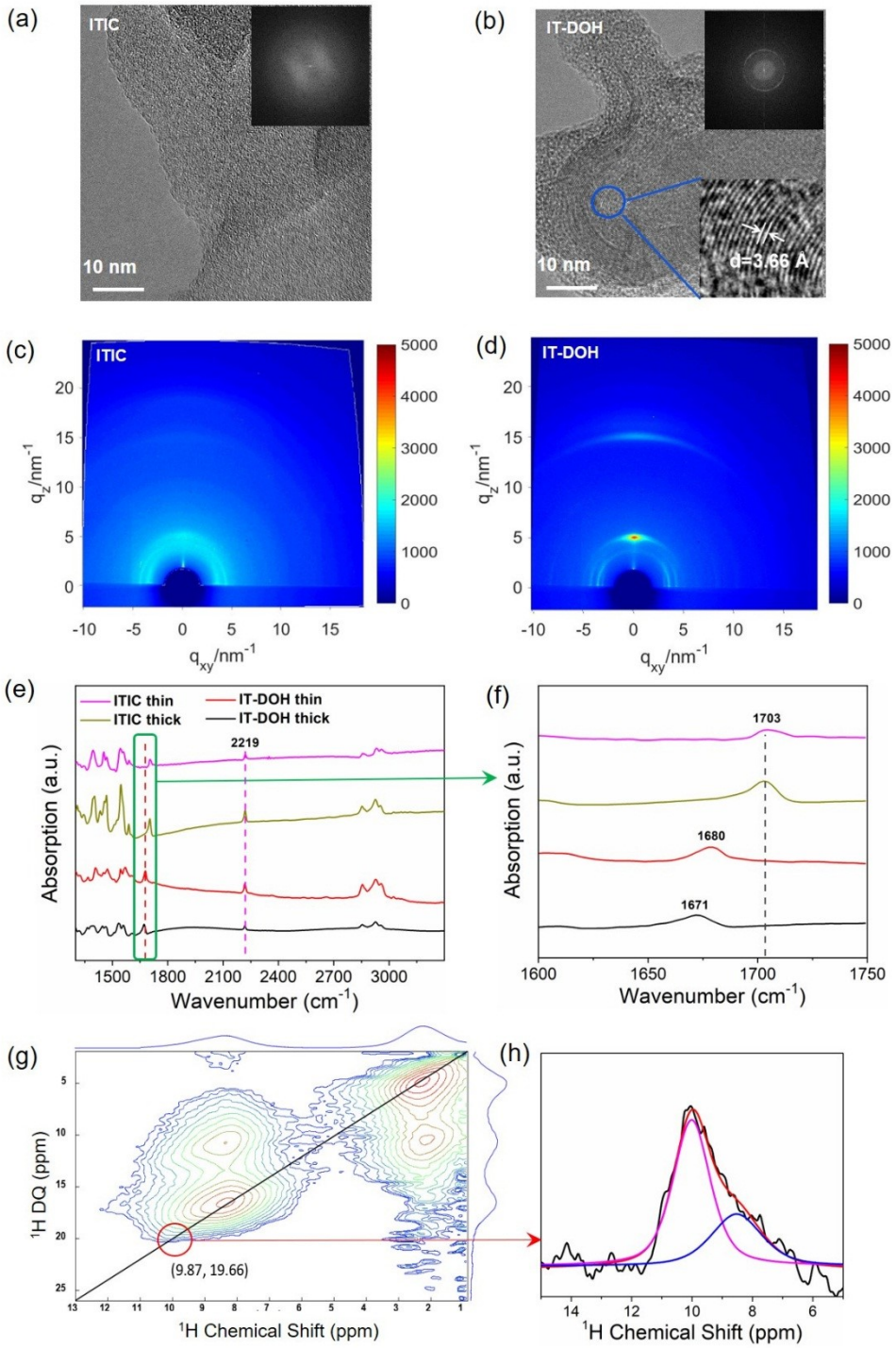

Fig. S5 (a, b) High-resolution TEM images and (c, d) GIWAXS patterns of ITIC and IT-DOH films. (e, f) FTIR absorption spectra of ITIC and IT-DOH thin and thick films prepared from chlorobenzene solutions of 3 and 12 mg mL^{-1}, respectively, by spin-coating. Reproduced with permission.[3] Copyright 2020 Wiley-VCH Verlag GmbH & Co. KGaA, Weinheim. (g) 2D ^{1}H-^{1}H DQ/SQ NMR spectrum of IT-DOH and (h) the correlative 1D spectrum.

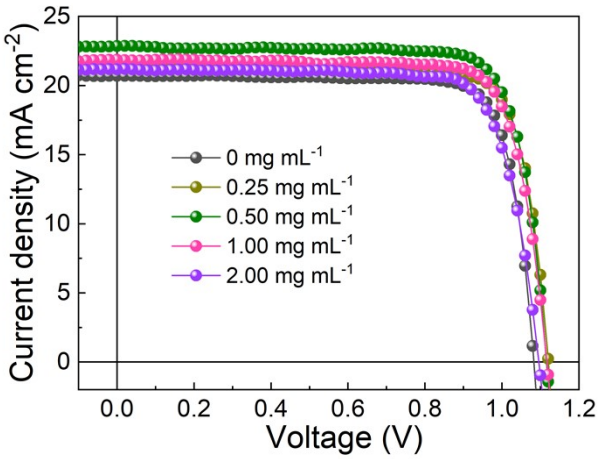

Fig. S6 J-V curves of CsFAMA-based PSCs with different IT-DOH concentrations in the anti-solvent.

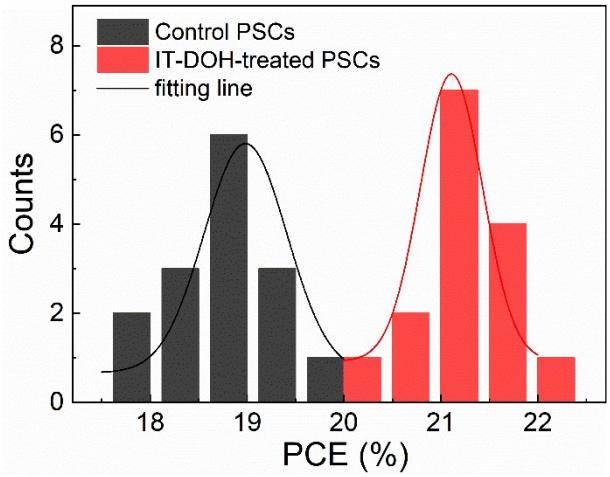

Fig. S7 Histogram of PCE values distribution for CsFA-based PSCs.

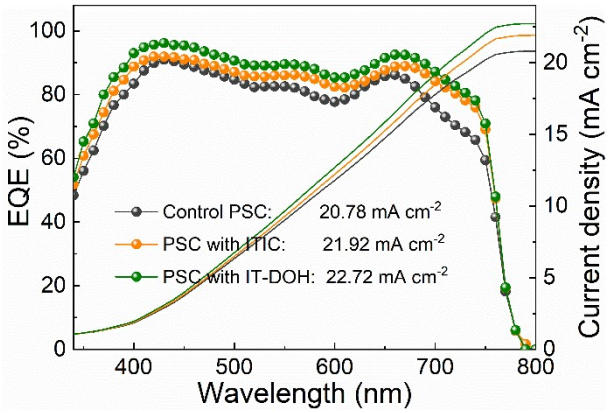

Fig. S8 EQE curves and integrated J_{sc} of CsFAMA-based PSCs without and with ITIC or IT-DOH treatment.

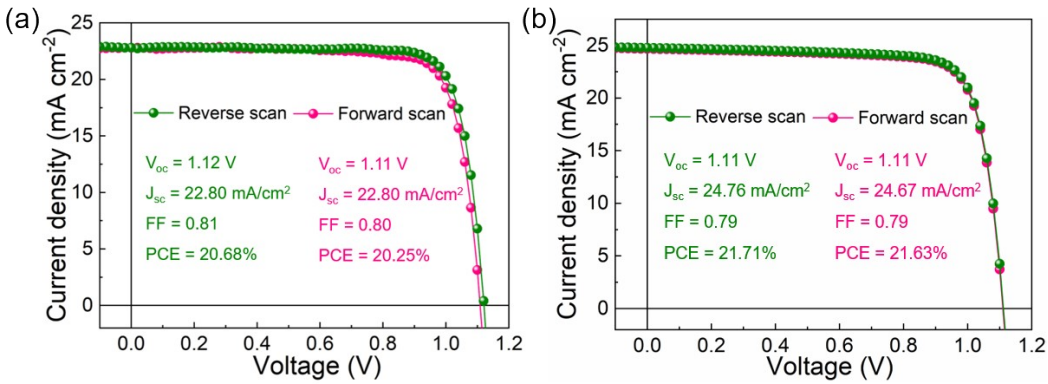

Fig. S9 J-V curves of IT-DOH-treated PSCs based on (a) the CsFAMA and (b) the CsFA perovskites, respectively, measured in both reverse and forward scanning directions.

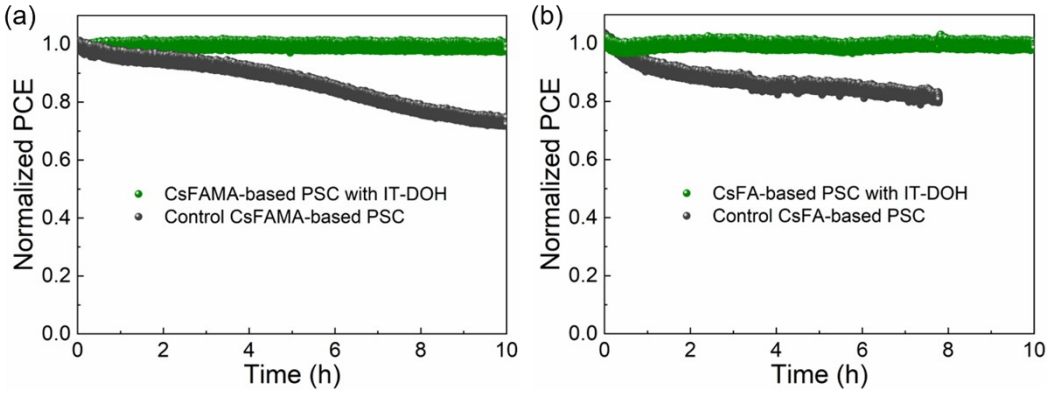

Fig. S10 MPP tracking of devices. One device was used for the test with (initial PCEs of 20.43% and 21.71% for CsFAMA- and CsFA-based PSCs, respectively) and without (initial PCEs of 19.08% and 19.85% for CsFAMA- and CsFA-based PSCs, respectively) IT-DOH treatment, respectively.

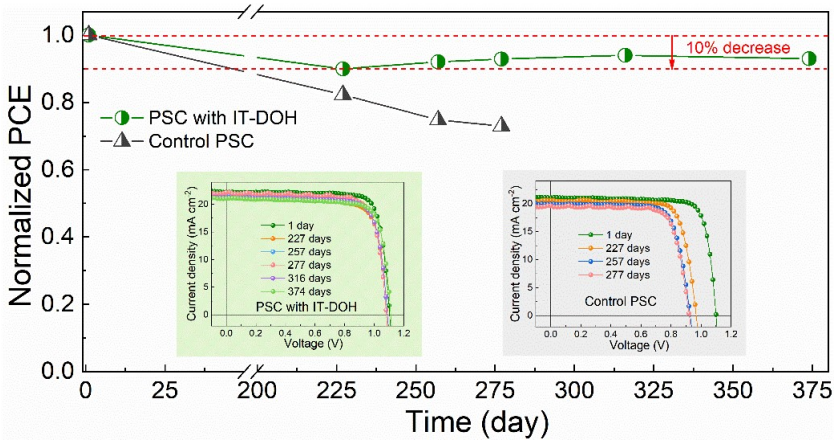

Fig. S11 Storage stability of CsFAMA-based devices; inset: typiacl J-V curves of PSCs. The data were collected from average values of four devices for each test. The devices were stored and tested in nitrogen-filled glove box with low water and oxygen content (both below 0.01 ppm) at room temperature.

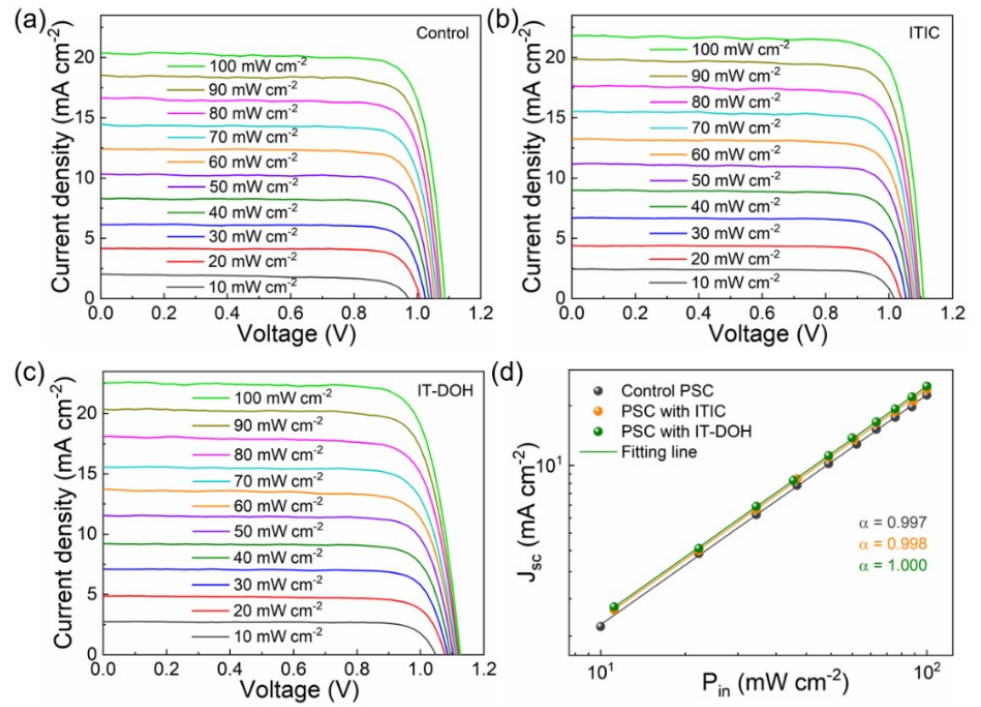

Fig. S12 J-V curves of (a) control, (b) ITIC-treated and (c) IT-DOH-treated PSCs measured under different light intensity. (d) Plots and fitting line of light intensity dependence of J_{sc} of PSCs. All devices are based on the CsFAMA perovskite.

Table S1. Binding energy values of Pb 4*f* for the control, ITIC-treated and IT-DOH-treated perovskite films based on the CsFAMA, respectively.

Sample	Pb 4*f* 5/2	Pb 4*f* 7/2
Control perovskite	143.72	138.87
ITIC-treated perovskite	143.56	138.70
IT-DOH-treated perovskite	143.30	138.43

Table S2. Peak center of steady-state PL of CsFAMA-based perovskite films with different treatments.

Sample	Peak center (nm)
Control perovskite	762.6
ITIC-treated perovskite	759.5
IT-DOH-treated perovskite	755.5

Table S3. Summary of TRPL lifetimes of CsFAMA-based perovskite films with different treatments.

Sample	τ_1 (ns)	τ_2 (ns)
Control perovskite	405.6	-
ITIC-treated perovskite	77.8	396.9
IT-DOH-treated perovskite	13.8	77.0

Table S4. Photovoltaic parameters of CsFAMA-based PSCs with different IT-DOH concentrations in anti-solvent.

Concentration of IT-DOH (mg mL^{-1})	V_{oc} (V)	J_{sc} (mA cm^{-2})	FF	PCE (%)
0.00	1.08	20.70	0.81	18.20
0.25	1.12	21.37	0.81	19.39
0.50	1.13	22.91	0.81	21.00
1.00	1.12	21.86	0.80	19.57
2.00	1.10	21.17	0.78	18.16

Table S5. Charge collection probability (*P*) of CsFAMA-based PSCs with different treatments.

Device	*P* (%)
Control PSC	94.2
PSC with ITIC	95.9
PSC with IT-DOH	96.8

Table S6. TPV decay lifetimes of CsFAMA-based PSCs with different treatments.

Device	τ (μs)
Control PSC	1.83
PSC with ITIC	2.96
PSC with IT-DOH	4.17

Table S7. Parameters fitted from EIS plots of CsFAMA-based PSCs with different treatments.

Device	R_s (Ω)[a]	R_{ct} (Ω)[b]	R_{rec} (Ω)[c]
Control PSC	68.5	176.0	29.5
PSC with ITIC	67.9	124.3	41.9
PSC with IT-DOH	68.2	72.4	80.4

[a] R_s is the series resistance of devices.

[b] R_{ct} is the charge transfer resistance at the interface of perovskite/ETL.

[c] R_{rec} is the recombination resistance of devices.

References

1. M. Feike, D. E. Demco, R. Graf, J. Gottwald, S. Hafner and H. W. Spiess, *J. Magn. Reson., Ser. A*, 1996, **122**, 214-221.
2. B. Li, Y. Xiang, K. D. G. Imalka Jayawardena, D. Luo, Z. Wang, X. Yang, J. F. Watts, S. Hinder, M. T. Sajjad, T. Webb, H. Luo, I. Marko, H. Li, S. A. J. Thomson, R. Zhu, G. Shao, S. J. Sweeney, S. R. P. Silva and W. Zhang, *Nano Energy*, 2020, **78**, 105249.
3. X. Liu, X. Wang, Y. Xiao, Q. Yang, X. Guo and C. Li, *Adv. Energy Mater.*, 2020, **10**, 1903650.